MONTHLY WEATHER REVIEW
VOLUME 95, NUMBER 4
APRIL 1967

SIMULATED CLIMATOLOGY OF A GENERAL CIRCULATION MODEL WITH A HYDROLOGIC CYCLE

II. ANALYSIS OF THE TROPICAL ATMOSPHERE

SYUKURO MANABE AND JOSEPH SMAGORINSKY

Geophysical Fluid Dynamics Laboratory, ESSA, Washington, D.C.

ABSTRACT

The thermal and dynamical structure of the tropical atmosphere which emerged from the numerical integration of our general circulation model with a simple hydrologic cycle is analyzed in detail.

According to the results of our analysis, the lapse rate of zonal mean temperature in the model Tropics is super-moist-adiabatic in the lower troposphere, and is sub-moist-adiabatic above the 400-mb. level in qualitative agreement with the observed features in the actual Tropics. The flow field in the model Tropics also displays interesting features. For example, a zone of strong convergence and a belt of heavy rain develops around the equator. Synoptic-scale disturbances such as weak tropical cyclones and shear lines with strong convergence develop and are reminiscent of disturbances in the actual tropical atmosphere. The humid towers, which result from moist convective adjustment and condensation, develop in the central core of the regions of strong upward motion, sometimes reaching the level of the tropical tropopause and thus heating the upper tropical troposphere. This heating compensates for the cooling due to radiation and the meridional circulation.

According to the analysis of the energy budget of the model Tropics, the release of eddy available potential energy, which is mainly generated by the heat of condensation, constitutes the major source of eddy kinetic energy of disturbances prevailing in the model Tropics.

CONTENTS

1. INTRODUCTION

This study is a continuation of the paper published under the same title in the December 1965 issue of the *Monthly Weather Review* [6]. In the previous study, the circulation of the model in the Tropics was analyzed rather superficially because we felt that it was excessively influenced by the artificial wall at the equator, a free-slip lateral boundary. However, further investigation of the results of the numerical integration, which was conducted after the publication of the previous paper, reveals that there are many interesting features of the tropical model atmosphere reminiscent of the actual atmosphere. For example, we are successful not only in simulating the tropical convergence zone or rainbelt (see fig. 1), but also the vertical thermal structure and some of the characteristic features of synoptic scale disturbances in the Tropics. It was decided therefore to perform a detailed analysis of the tropical atmosphere of the model, and to publish the results despite the possible influence of the equatorial wall.

Because of the inadequate observational network, quantitative description and understanding of the thermal and dynamical structure of the tropical atmosphere remain unrefined. For example, it is not clear whether the kinetic energy of tropical disturbances is maintained mainly by barotropic processes or through the release of potential energy. Malkus [5] has commented:

"In contrast to the middle-latitude cyclones, tropical disturbances do not contain fronts, but form and live their lives entirely within tropical air (except for the escaped hurricane). Thus, they are not able to feed upon stored potential energy in pre-existent horizontal temperature contrasts, but must either create their own energy by differential latent heat release, or draw their kinetic energy and momentum from other scales of motion. The relative importance

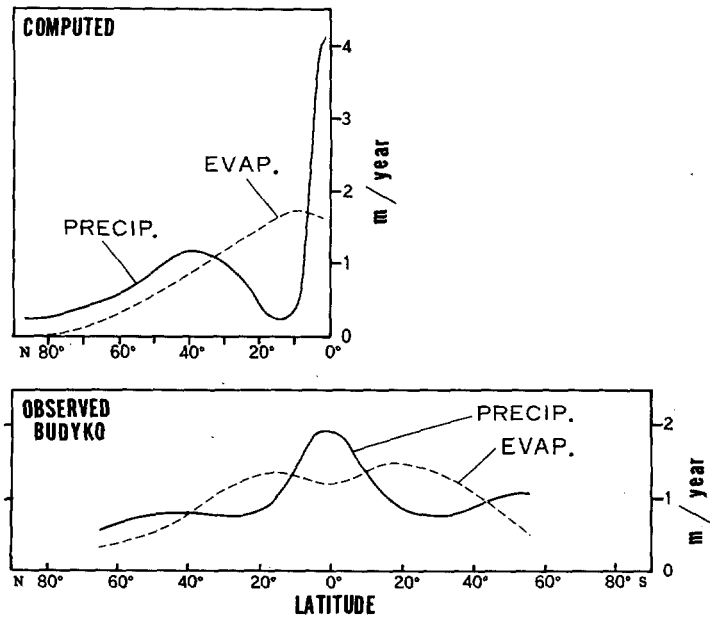

FIGURE 1.—Above, the latitudinal distribution of precipitation and evaporation obtained from the model. Below, observed distributions estimated by Budyko [1] are shown in units of m./yr.

of these processes is not well known, except in deep disturbances of wet seasons where the major energy source is demonstratively condensation."

A final answer to this question must await a careful analysis of the dynamics of the tropical disturbances and a theoretical study of their instability characteristics. Recently Lipps [3] suggested the possibility of the formation of easterly waves through barotropic processes. In this paper, we shall conduct a detailed study on the mechanism for maintaining the eddy kinetic energy in the model Tropics. It is hoped that this study will prove useful both in speculating on the behavior of the disturbances in the actual Tropics and in designing a future observational system for the tropical atmosphere.

Another interesting feature that awaits clarification is the mean thermal structure of the tropical atmosphere. Examination of the vertical distribution of temperature reveals that the lapse rate is super-moist-adiabatic in the lower troposphere, and sub-moist-adiabatic above the 400-mb. level. It is generally accepted that this thermal structure of the tropical atmosphere is a very important factor in determining the development of tropical cyclones. In this study, we shall perform an analysis of the heat balance and thermal structure of the model for the Tropics emerging from the numerical integration.

As we explained in our previous paper, one of the most serious difficulties in designing a numerical model of the general circulation is in the parameterization of the moist convection. In view of our ignorance of the interaction of small-scale convection with the large-scale fields of motion and temperature, we adopted an extremely simple system of moist convection, but one that nevertheless possesses some of the essential characteristics of actual convection. The basic assumptions adopted for this system of moist convection are as follows:

a. If air is saturated and the lapse rate is super moist-adiabatic, the free convection is strong enough to make the equivalent potential temperature and relative humidity uniform in the unstable layer.
b. The sum of potential, internal, and latent energy is conserved during the convective adjustment. (See [6] for further details.)
c. The criterion for saturation is 100 percent relative humidity.

There is no doubt that this simplified system of moist convection significantly influenced the general circulation of the model in the Tropics. It is therefore essential that the present results be interpreted in light of the system's properties.

In order to investigate the role of condensation in maintaining the thermal and dynamical structure of the model for the Tropics, a detailed comparison has been made between the results obtained from both moist and dry general circulation model integrations (see [6] and [15]). In the dry general circulation model, the effect of phase transitions of water substance was completely neglected. However, the lapse rate was adjusted back to the moist adiabatic value whenever it exceeded this critical value to prevent static instability. It turned out that this comparison between the dry and moist model equilibrium states is extremely useful for understanding the tropical atmosphere of the moist model.

2. ZONAL MEAN PROPERTIES

Figure 2.1 shows the vertical distribution of temperature in the tropical troposphere of the moist model. We see that the lapse rate of the lower troposphere is super-moist-adiabatic, and that of the upper troposphere (above the 400-mb. level) is sub-moist-adiabatic, in qualitative agreement with observation. However, the super-moist-adiabatic lapse rate of the lower troposphere is somewhat exaggerated in the model atmosphere, probably because of the shortcomings of the convective adjustment scheme. In our model, the critical relative humidity for the onset of moist convection was assumed to be 100 percent, whereas without doubt it is less than 100 percent in the actual atmosphere. This simplifying assumption may be responsible for both insufficient convective activity and for creating too unstable a lapse rate near the earth's surface. In the dry model atmosphere, where convective adjustment is made whenever the lapse rate becomes super-moist-adiabatic, the lapse rate turned out to be neutral (moist-adiabatic) in the tropical troposphere.

The mechanism for maintaining the stable lapse rate in the upper troposphere was recently discussed by Riehl [12]. He analyzed the measurements of the flux of long-wave radiation which were made over the Caribbean Sea using the radiometersonde developed by Suomi and Kuhn

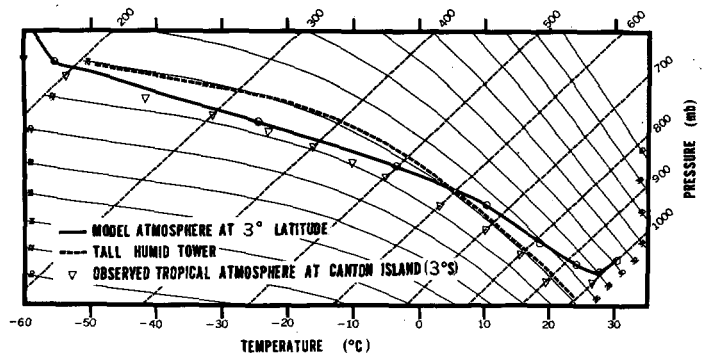

FIGURE 2.1.—Solid line shows the vertical distribution of temperature in the model Tropics (3° latitude), ▽ symbol shows the annual mean temperature (1962) at Canton Island (3° S.). Dotted line shows one example of the vertical distribution of temperature in the "humid tower".

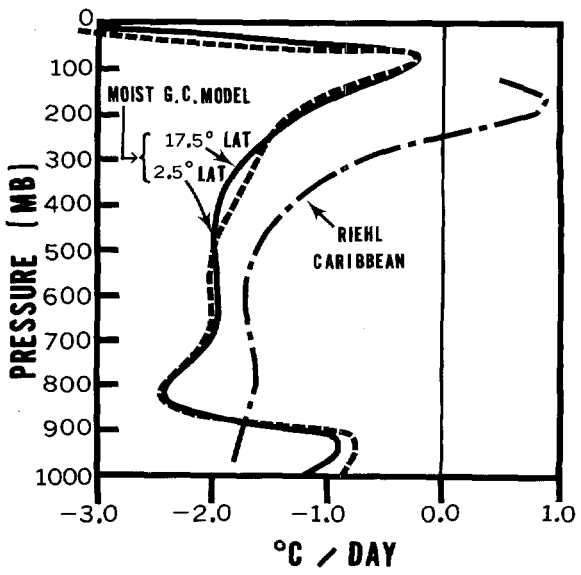

FIGURE 2.2.—Vertical distribution of the temperature change due to long-wave radiation over the Caribbean Sea (Riehl [12]). The distributions of the corresponding quantity at 2.5° latitude and 17.5° latitude in the moist model Tropics are also shown.

[16]. According to his results, the radiative cooling in the upper troposphere is significantly smaller than that obtained by London [4] for tropical latitudes. Around the 200-mb. level, the measurements even indicate the existence of a heated layer. He speculated that this heated layer results from the absorption of upward long-wave radiation by trapped haze or cirrus invisible from the ground, which may exist just below the equatorial tropopause. Based upon these results, he suggested that this heating may be responsible for the stable layer which is observed in the upper troposphere of the Tropics. Since the effect of such absorbers is not incorporated in our model, the heated layer does not appear in our results, as figure 2.2 shows. Examination of the tropical atmosphere produced by the dry general circulation model reveals that the lapse rate becomes stable only above level 3 ($P/P_*=0.189$). Below this level, the lapse rate is neutral (moist-adiabatic), in contrast to the case of the moist model. These results suggest that the temperature change caused by the large-scale motion field, which is influenced by the heat of condensation, seems to be an important factor in maintaining the stable layer in the upper tropical troposphere of the moist model.

Figure 2.3 shows the vertical distribution of various heat balance components at 3° latitude of the moist model simulation. (For comparison the corresponding distributions for the dry model are shown.) We see that the cooling due to radiation (the net effect of solar and long-wave components) and the meridional circulation is compensated for by the heating due to condensation and moist convection. As we shall see in the next section, the convective adjustment in the model Tropics sometimes reaches the upper troposphere, where it releases heat of condensation (see fig. 12.C.1 of [6]). This is in qualitative agreement with the results of a study of the heat balance of the tropical atmosphere conducted by Riehl and Malkus [13]. As we explained in the preceding paragraph, more recent results of Riehl [12] suggest that long-wave radiation does not always have a cooling effect. However, figure 2.2, which includes the result of Riehl [12], indicates the existence of cooling from long-wave radiation below about the 250-mb. level.

One of the interesting features of the moist atmosphere is the development of an intense direct meridional circulation in the Tropics. In table 2.1, the intensities of the circulation are shown for both the dry [1] and moist models. Estimates of its intensity in the actual atmosphere, obtained by Palmén and Vuorela [11] and Mintz and Lang [8], are added to the same table for comparison. This table clearly shows that the condensation process contributed significantly to the intensification of the tropical cell of the model atmosphere. In the dry model, the intensities of the direct cell in the Tropics and that of the indirect cell in the middle latitudes are about equal. On the other hand, the former is stronger than the latter in

[1] The value for the zonal mean of the meridional component of wind, which is shown in the lower half of figure 4.B.2 of [15] is only 1/10 the correct value. (See correction on p. 528, Aug. 1966 issue, *Monthly Weather Review*.)

TABLE 2.1.—*Approximate intensity of meridional circulation (Units: 10^{12}gm./sec.)*

	Calculated		Observed		
	Dry Model	Moist Model	Palmén and Vuorela [11]	Mintz and Lang [8]	
	Annual mean	Annual mean	Winter	Winter	Summer
Direct cell in the Tropics	52	140	230	85	40
Indirect cell in middle latitudes	46	23	30	27	30

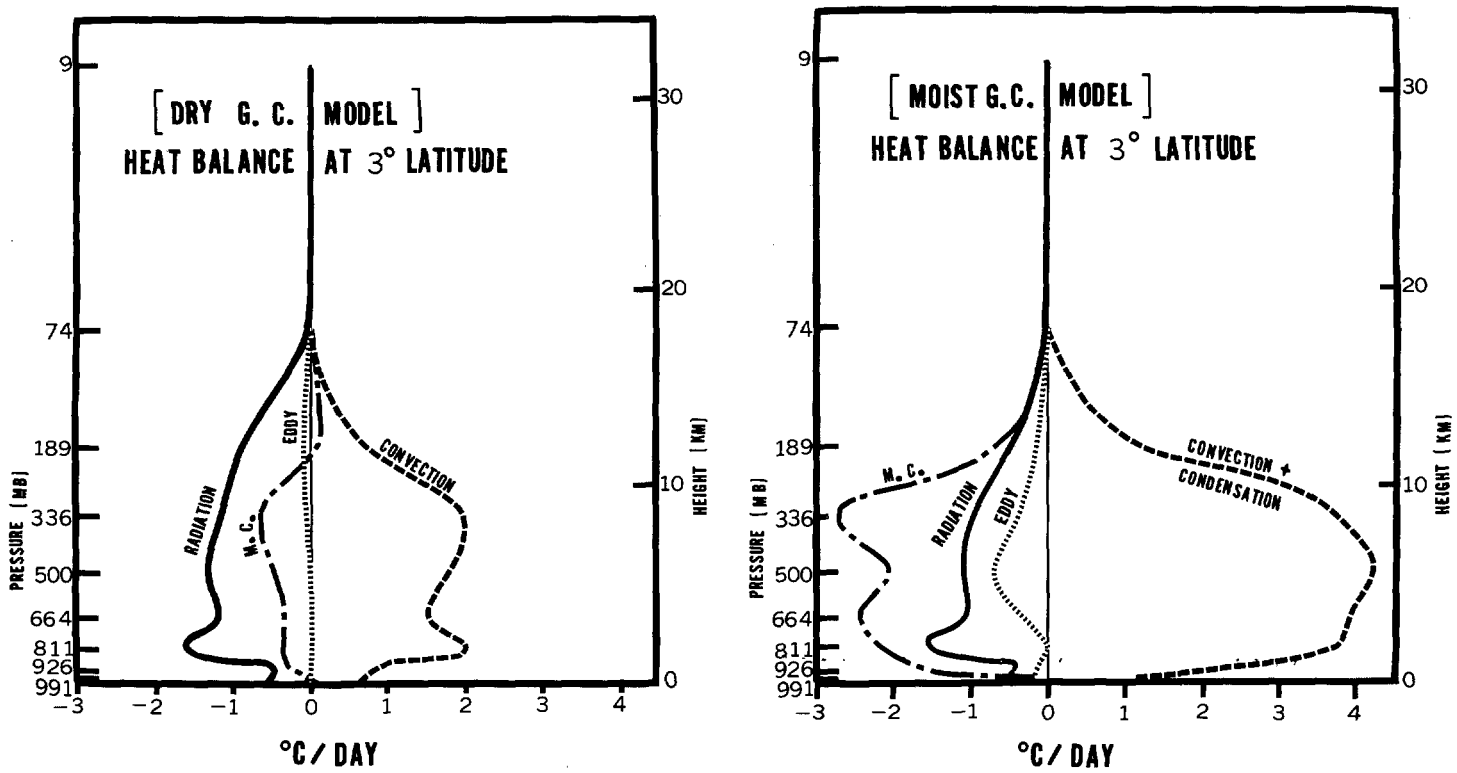

FIGURE 2.3.—Vertical distributions of temperature change due to meridional circulation, radiation, large-scale eddies, and convective adjustment and condensation (moist model only), are shown for both dry and moist model atmospheres.

the moist model atmosphere, in qualitative agreement with observations ([8] and [11]). Although the intensity of the direct cell is somewhat smaller than the estimate obtained by Palmén and Vuorela [11] for winter, it is significantly larger than that obtained by Mintz and Lang [8]. (Note that the annual mean insolation was adopted for our study.) A comparison between figure 12.B.3 and figure 12.B.4 of our previous paper [6] shows that in the Tropics the southward transport of water vapor by the direct cell is much larger in the model atmosphere than in the actual atmosphere. Therefore, it seems that the direct cell in the moist model is exaggerated. This results in an increase of relative angular momentum in the upper troposphere of the subtropics and may be responsible for the abnormal intensity of the subtropical jet stream which appears in the moist model atmosphere. The latitude of maximum westerlies in the moist model atmosphere is about 27°, which is farther south than in the actual atmosphere. The insulated free-slip wall at the equator may be partly responsible for this exaggeration of the intensity of the direct cell, because it tends to anchor the tropical rainbelt at a specific latitude, i.e., the equator.

Finally we shall briefly describe the distribution of relative humidity in the model for the Tropics. According to figure 2.4[2] which shows the latitude-height distribution of relative humidity in the actual and the model Tropics, the relative humidity in the model Tropics is at a maximum near the earth's surface, and decreases with increasing altitude up to the 400-mb. level. It increases again and reaches a maximum value around the 200-mb. level. In the tropical stratosphere (above the 20-km. level), the relative humidity is less than 10 percent. These features of the vertical distribution of relative humidity are in qualitative agreement with observation (shown in the lower part of fig. 2.4). It should be mentioned that measurements by Mastenbrook [7] at Kwajalein atoll show similar characteristics. As figure 8.7 of the previous paper [6] indicates, the humidity in the model atmosphere is uniformly high near the earth's surface because of evaporation from the underlying wet surface. The variability of relative humidity increases with increasing altitude, as a result of the field of strong vertical motion. Because of this variability, the zonal mean humidity decreases with increasing altitude up to the 400-mb. level.

3. SYNOPTIC MANIFESTATIONS

In figure 3.1, the streamlines of the moist model simulation at level 5 ($P/P_*=0.500$), level 7 ($P/P_*=0.811$), and level 9 ($P/P_*=0.991$) are contrasted against those of the dry model. Near the earth's surface, small-scale eddies predominate in the Tropics in the moist model, whereas the flow pattern is relatively smooth in the dry model. It should be recalled that the equatorial grid size is 320 km. Near the earth's surface, air generally

[2] Figure 7.3 of [6], which corresponds to the present figure 2.4 and shows the distribution of relative humidity, has an error. As figure 2.4 shows, the contour line in the upper left corner of the computed distribution should be 0.1 percent.

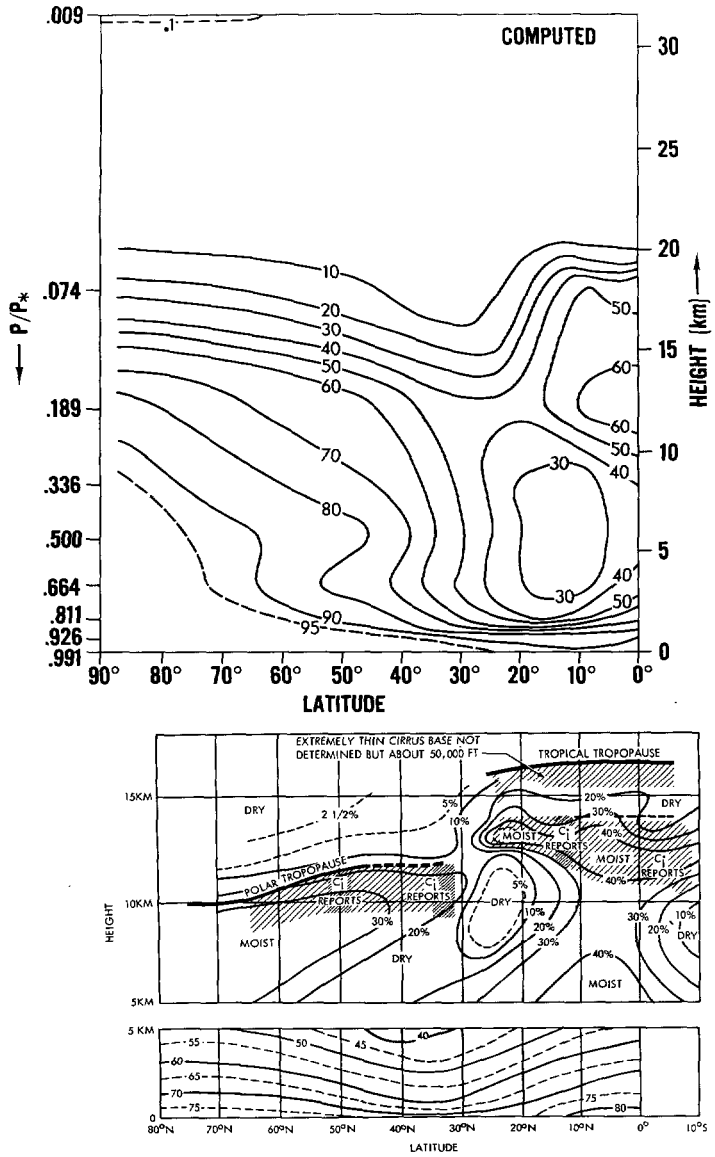

FIGURE 2.4.—Latitude-height distributions of relative humidity (in percent): Upper section—for the model atmosphere; lower section—for the actual atmosphere for the summer season (by Murgatroyd [9], Telegadas and London [17]).

converges toward the Tropics and easterlies predominate. Above the 500-mb. level of the moist model atmosphere, westerly flow penetrates into very low latitudes. This situation is implied by the very shallow layer of tropical easterlies shown in the upper left corner of figure 6.1 of [6], and is reminiscent of the winter situation in the actual atmosphere.

Figure 3.2 shows a time sequence of the surface streamlines of the moist model atmosphere. In the lower right part of the streamline field on the 175th day of integration, one can see a weak tropical cyclone. This cyclone can also be identified in the maps of the 174th and 176th days. However, it is hardly identifiable on the 173d and 177th days. This figure indicates that many of the disturbances in the model Tropics change very rapidly, and have a short lifetime of 1 to 3 days. Figure 3.2a shows how the convergence line, which evolved into the cyclone mentioned above, was formed. The hourly variations of the wind along the line segment AB (see 175th day map of fig. 3.2) are shown for the 24-hr. period starting on the 173d day. We see that the line of convergence developed gradually during this 1-day period.[3] Such lines of convergence or sharp shear lines predominate in the model of the Tropics, in qualitative agreement with the actual Tropics. Since the line of convergence sometimes coincides with the equatorial wall, it is probable that its location is influenced by this free-slip lateral boundary. However, the convergence line often deviates from the wall, for example on the 177th day.

In order to examine the correspondence between the streamline field and the vertical motion, the area of upward motion at level 7½ ($P/P_*=0.874$) is shaded on the streamline map of the 175th day of the numerical integration (see fig. 3.2). The actual magnitude of vertical P-velocity is shown in figure 3.3. According to these figures, upward motion develops above surface synoptic disturbances, such as a convergence line or a weak cyclone. Near the center of upward motion, the air is very often saturated and the magnitude of vertical velocity very large. Figure 3.4 shows maps of typical vertical P-velocity at level 5½ ($P/P_*=0.583$) of both dry and moist model simulations for the entire hemisphere. From these we can see that intense small-scale vertical motion is missing from the tropical atmosphere of the dry general circulation simulation. Therefore, it is clear that the synoptic-scale disturbances accompanied by strong vertical motion are generated in conjunction with condensation processes.

In order to further clarify the characteristic structure of these disturbances, the tropical cyclone mentioned earlier was analyzed in detail. Cross-sections of relative humidity, vertical P-velocity, and temperature anomaly from zonal mean are displayed in figure 3.5. The locations of the cross sections AB and CD are indicated in figure 3.2 (175 days). Figure 3.6 is an enlarged version showing the pressure distribution. Examination of these figures reveals the following characteristics of this cyclone:

a. Strong upward motion predominates in the tropical cyclone (or on the lines of convergence) as a result of the self-amplification of vertical motion by the condensation process.
b. A tall humid tower with moist-adiabatic lapse rate develops in the area of strong upward motion (see also fig. 2.1). Sometimes this tower of convective adjustment reaches all the way up to the tropical tropopause (see fig. 8.7 of [6]).
c. In this humid tower, a warm temperature anomaly develops in the upper troposphere, i.e., the humid core has a warm-core structure in the

[3] In order to extract the hourly detail of the evolution of wind vector across the shear line, the numerical integration was repeated from the 103d day. However this was done a couple of years after the original integration, and the numerical model had been slightly modified. The result is therefore not an exact duplicate, but the two are similar enough for the above purpose.

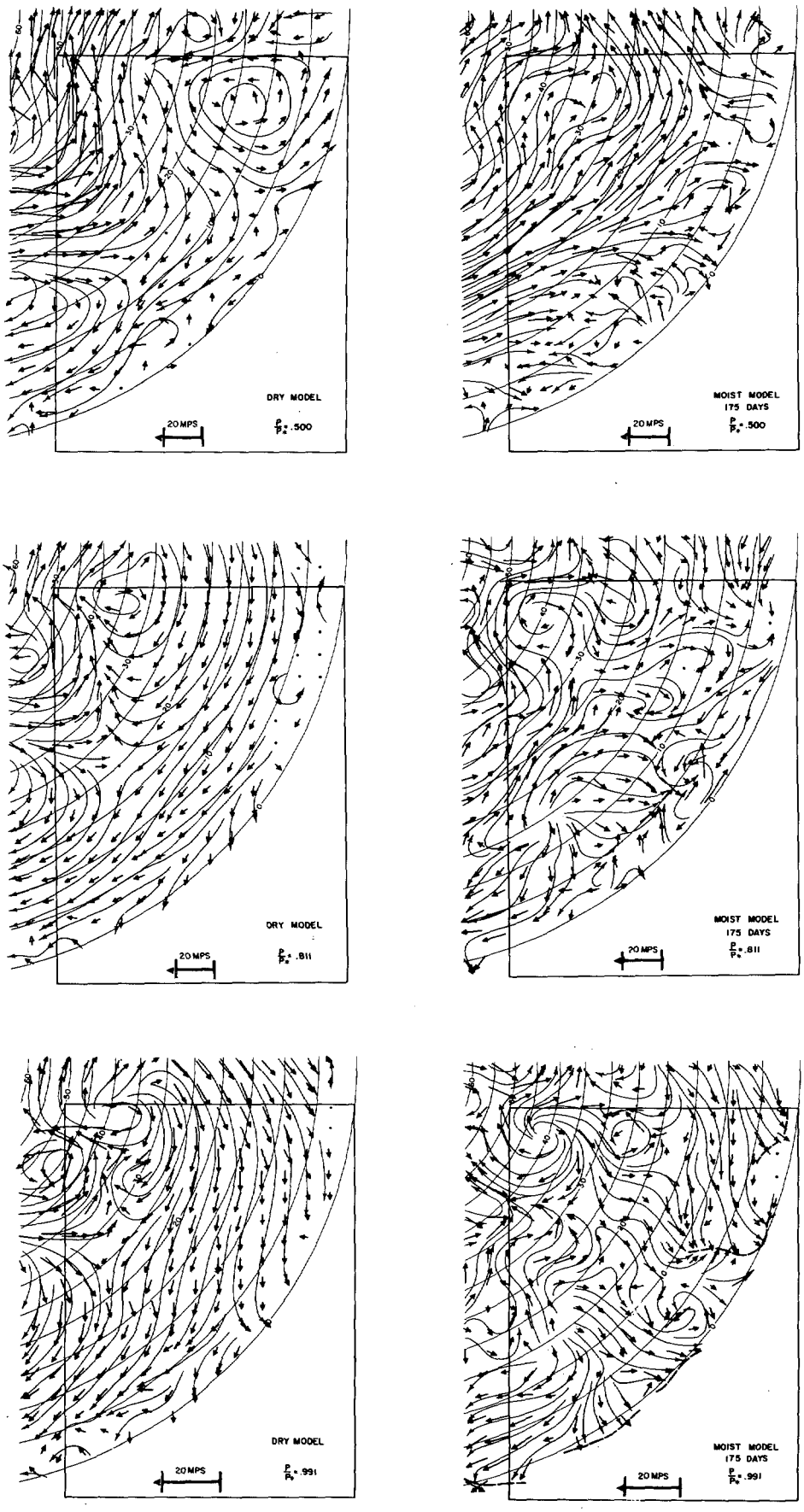

FIGURE 3.1.—Streamlines at level 5 ($P/P_* = 0.5$), at level 7 ($P/P_* = 0.811$), and at level 9 ($P/P_* = 0.991$) in both dry and moist atmospheres, are shown. Maps of the 175th day (moist model) and of the 259th day (dry model) of time integration were chosen for this figure. Wind vectors have their tail at the grid point; the length of the vector (excluding arrowhead) is proportional to the wind speed. Note the scale for wind vectors at level 9 is different from that at higher levels.

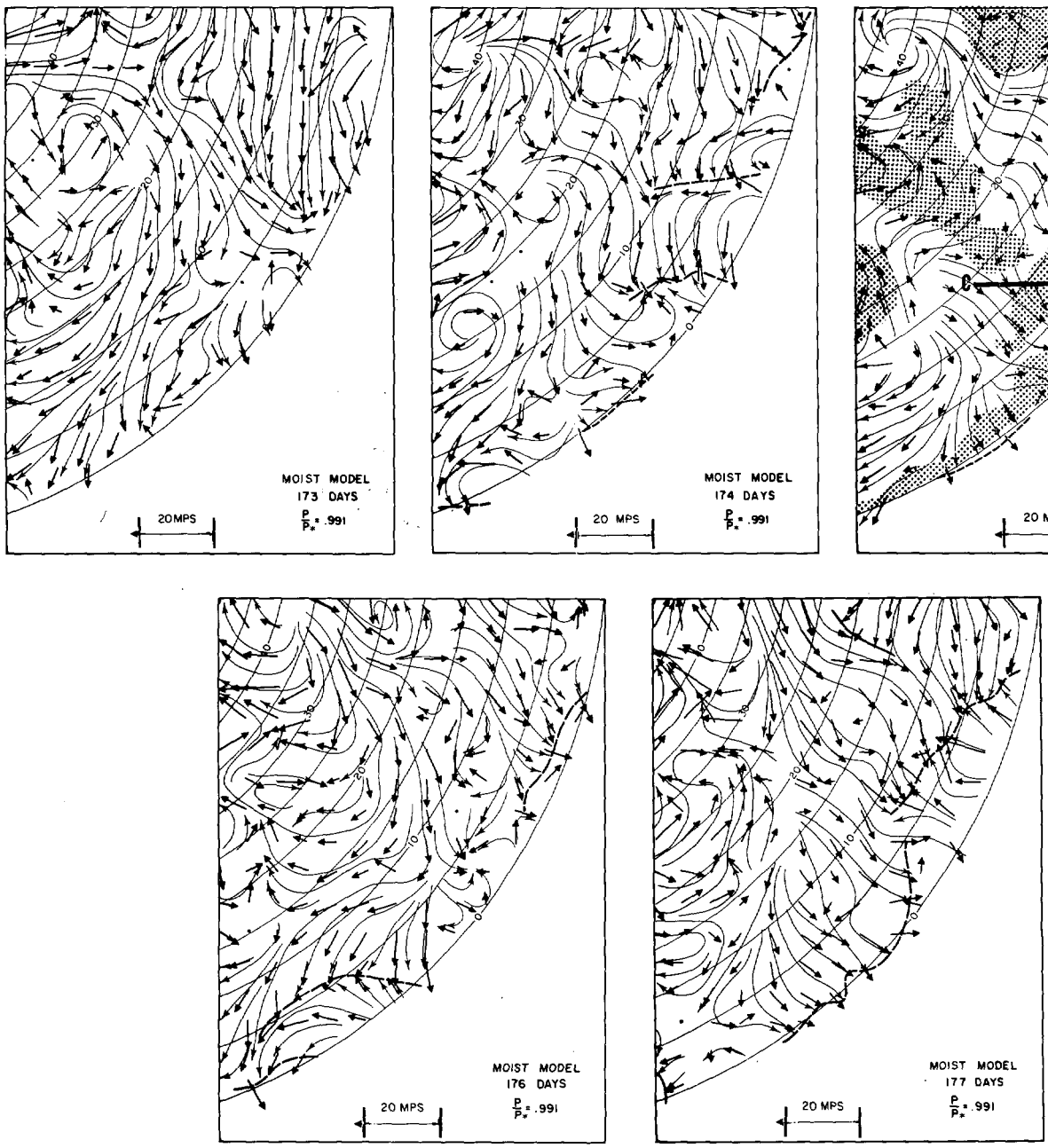

FIGURE 3.2.—The maps of streamlines at level 9 ($P/P_*=0.991$) on the 173d, 174th, 175th, 176th, and 177th days of numerical integration of the moist model are shown. Area of upward motion at level 7½ ($P/P_*=0.874$) are shaded in 175th day map. Lines AB and CD in 175th day map indicate the locations of cross sections shown in figure 3.5. Wind vectors have their tail at the grid point; the length of the vector (excluding arrowhead) is proportional to wind speed.

upper troposphere and a cold-core structure near the earth's surface.

d. The lower-level pressure gradients in the equatorial region are considerably smaller than those at higher latitudes, whereas the winds are only slightly less on the average.

As we pointed out in Section 2, the mean lapse rate of the tropical model atmosphere is super-moist-adiabatic in the lower tropical troposphere, and sub-moist-adiabatic in the upper tropical troposphere (above 400-mb. level) in agreement with observation. Since the convective tower creates a neutral lapse rate such that the sum of total potential energy and latent energy is conserved (see Introduction), it usually creates as a consequence a warm-core structure in the upper troposphere and cold-core structure near the earth's surface. This thermal structure of the tropical disturbance is responsible for the maximum release of eddy potential energy in the upper troposphere of the model Tropics, which we shall discuss in the next section. In the dry model, the warm-core structure does

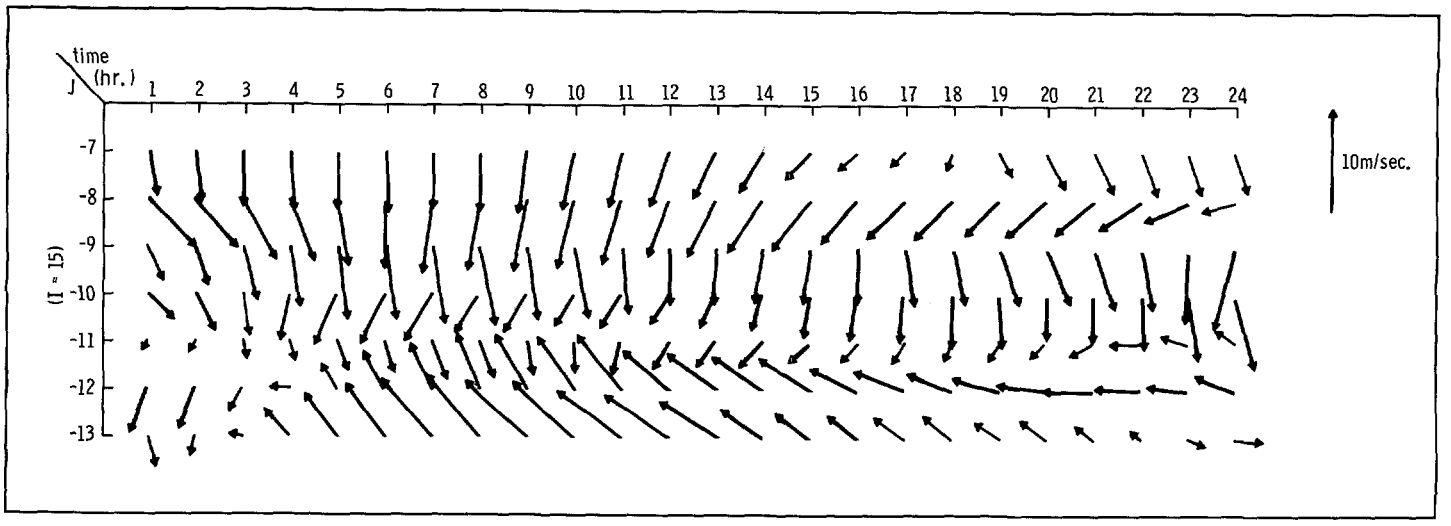

FIGURE 3.2.a.—Evolution of wind at level 9 ($P/P_* = 0.991$) along the line segment AB indicated in 175th day map of figure 3.2. The time period is from the 173d to the 174th day. The length of wind vector (excluding arrowhead) is proportional to wind speed.

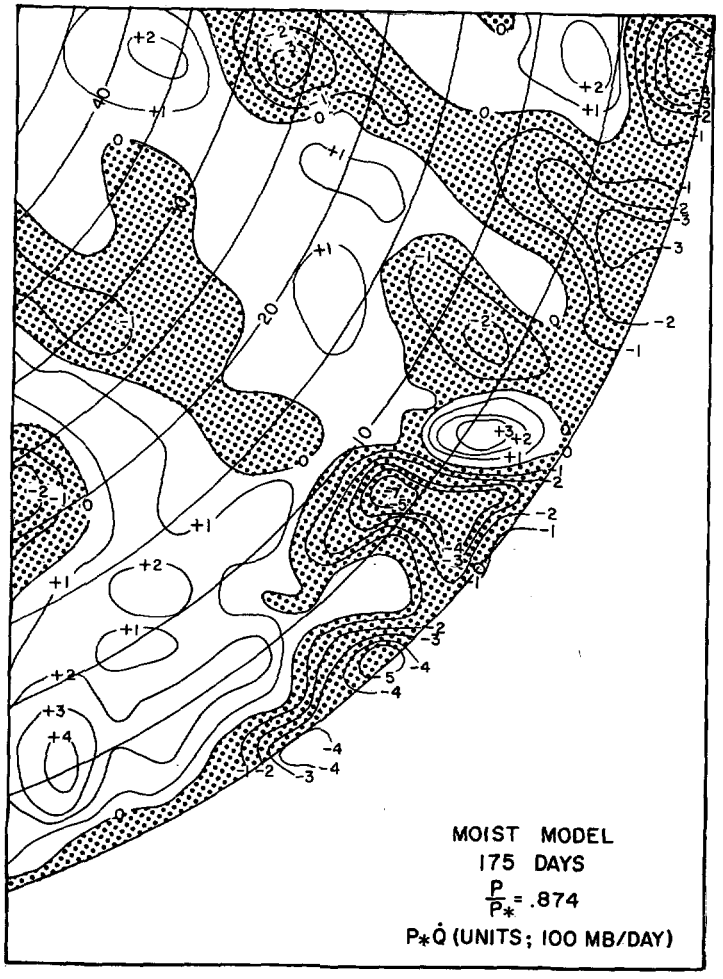

FIGURE 3.3.—Map of vertical P-velocity at level 7½ ($P/P_* = 0.874$) on 175th day of integration. Contour interval, 100-mb./day. The area of upward motion is shaded. The vertical velocity is effectively the average of the 3-hr. period preceding the 175th day.

not appear because the very efficient convective adjustment results in a neutral lapse rate everywhere. As we explained in the previous section, the convective humid towers provide the most important heat sources in the upper troposphere of the model atmosphere. Therefore, such a tower may be likened to the clusters of "hot towers" in the actual atmosphere, which were observed and emphasized by Riehl and Malkus [13]. We quote:

"In the ordinary, small-size trade cumuli, buoyancy is wasted away by mixing with the surroundings; few of their tops penetrate more than half a kilometer into the dry air above the inversion. But within the general rain area of equatorial disturbances, there are imbedded central cores in the penetrative giant cumulonimbus which are protected from dilution by the large cross section of towers. In this way, the high heat content, ocean-exposed air of subcloud layer can be pumped to great height to balance the heat losses, and provide the calculated exports."

Yanai [19] distinguishes three stages in the process of tropical cyclone formation based upon his analysis of tropical disturbances. The first stage is an intense easterly wave. In the second stage, a warming of the upper troposphere occurs from the release of heat of condensation, resulting in a progressive downward warming of the cold core. The third stage is the development into a mature tropical cyclone after the core is completely warm. The relatively short characteristic lifetime of the simulated moist model tropical disturbances, having a cold core near the earth's surface and a warm core aloft, suggests that these disturbances do not go beyond the second stage defined by Yanai. They correspond more to the immature atmospheric counterpart. One can speculate upon various possibilities for the absence of mature hurricanes in the models, i.e.,

a. It is impossible to represent the structure of the central part of a hurricane by the resolution of our grid system (see the last paragraph of Section 5).
b. The sensible heat transferred from the sea surface may be an important factor which is effective in

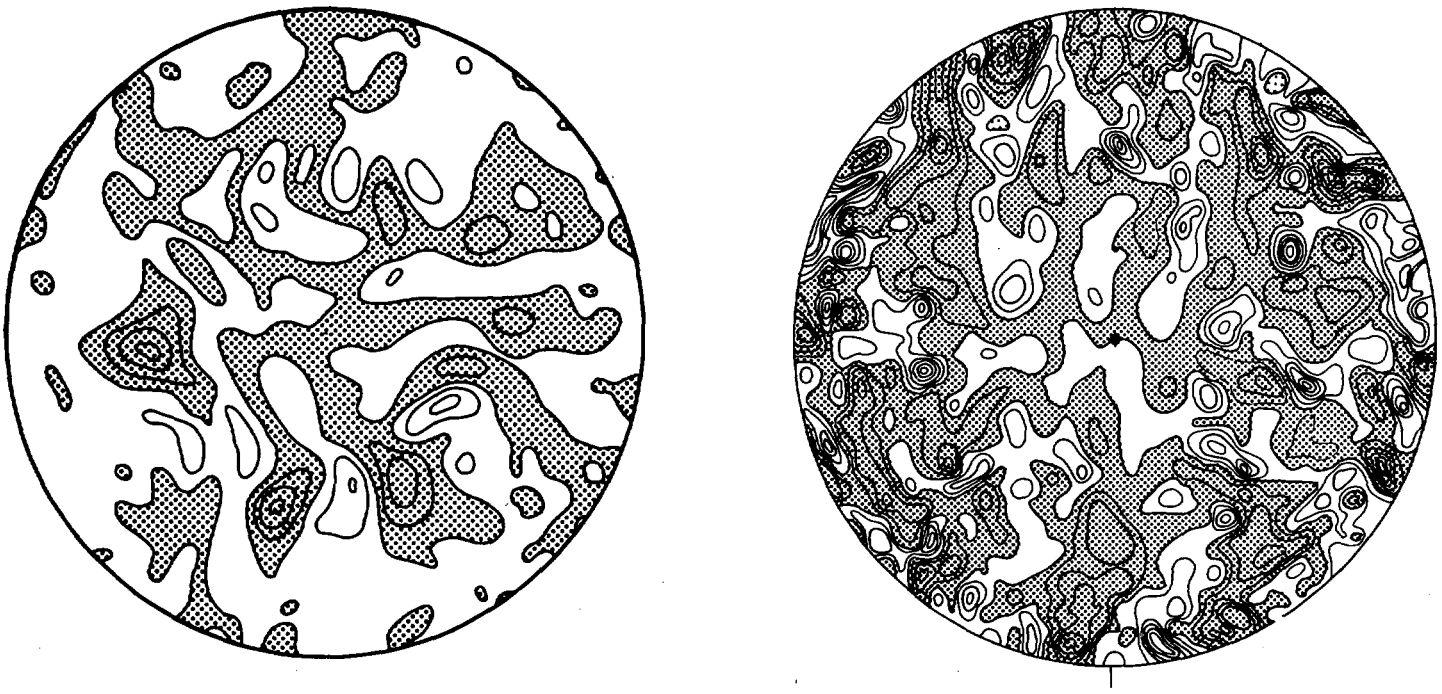

FIGURE 3.4.—Maps of vertical P-velocity at level 5½ ($P/P_*=0.583$) for both dry and moist models. Contour interval, 100-mb./day. The vertical velocity is effectively the average of the 3-hr. period preceding the day indicated.

eliminating the cold core near the earth's surface and which is missing in the moist model.

c. It is well known that tropical disturbances are less active during winter when the layer of easterlies is shallow than during the summer when it is deep. The layer of easterlies of the Tropics in this model is shallow.

d. A mature tropical cyclone might be suppressed if the delicate balance between the latent heat source of energy and frictional dissipation were not properly represented. Both of these mechanisms are highly parameterized in the model, and so of questionable fidelity.

Nevertheless, the commonly occurring immature disturbances in the model Tropics are quite effective in maintaining the tropical energy budget within the context of the hemispheric general circulation. This suggests that the relatively rare mature cyclone or hurricane does not play a cruicial role in maintaining the energy balance of the general circulation.

4. EDDY ENERGY BUDGET

In this section, we shall investigate how the kinetic energy of the tropical disturbances is maintained. According to figure 4.1, which shows the latitudinal distributions of eddy kinetic energy, the eddy kinetic energy in the Tropics of the moist model is much larger than that of the dry model. In order to clarify the reason for this difference, the latitude-height distribution of the rate of the conversion of eddy available potential energy to eddy kinetic energy $\left(\overline{-\omega'\alpha'}^{\lambda}\right)$ in the moist model atmosphere is compared with that in the dry model atmosphere in figure 4.2 (see the Appendix for an explanation of notation). The former has a maximum rate of conversion in the Tropics as well as in middle latitudes, whereas the latter lacks the tropical maximum. It is interesting that a region of negative conversion of eddy available potential energy appears in the subtropics of the moist model atmosphere. In the lower part of figure 4.3, the latitudinal distribution of the conversion of eddy available potential energy

$$-\frac{1}{g}\int_0^{P_*}\overline{\omega'\alpha'}^{\lambda}\,dP$$

in the moist atmosphere is contrasted with that of the transfer of zonal kinetic energy into eddy kinetic energy, i.e.,

$$(K_Z\cdot K_E)=-\frac{1}{g}\int_0^{P_*}\left[\overline{u'v'}^{\lambda}\cos\theta\,\frac{1}{a}\frac{\partial}{\partial\theta}(\bar{u}^{\lambda}\sec\theta)+\overline{\omega'u'}^{\lambda}\frac{\partial\bar{u}^{\lambda}}{\partial P}\right]dP \quad (4.1)$$

According to this figure, the conversion of eddy available

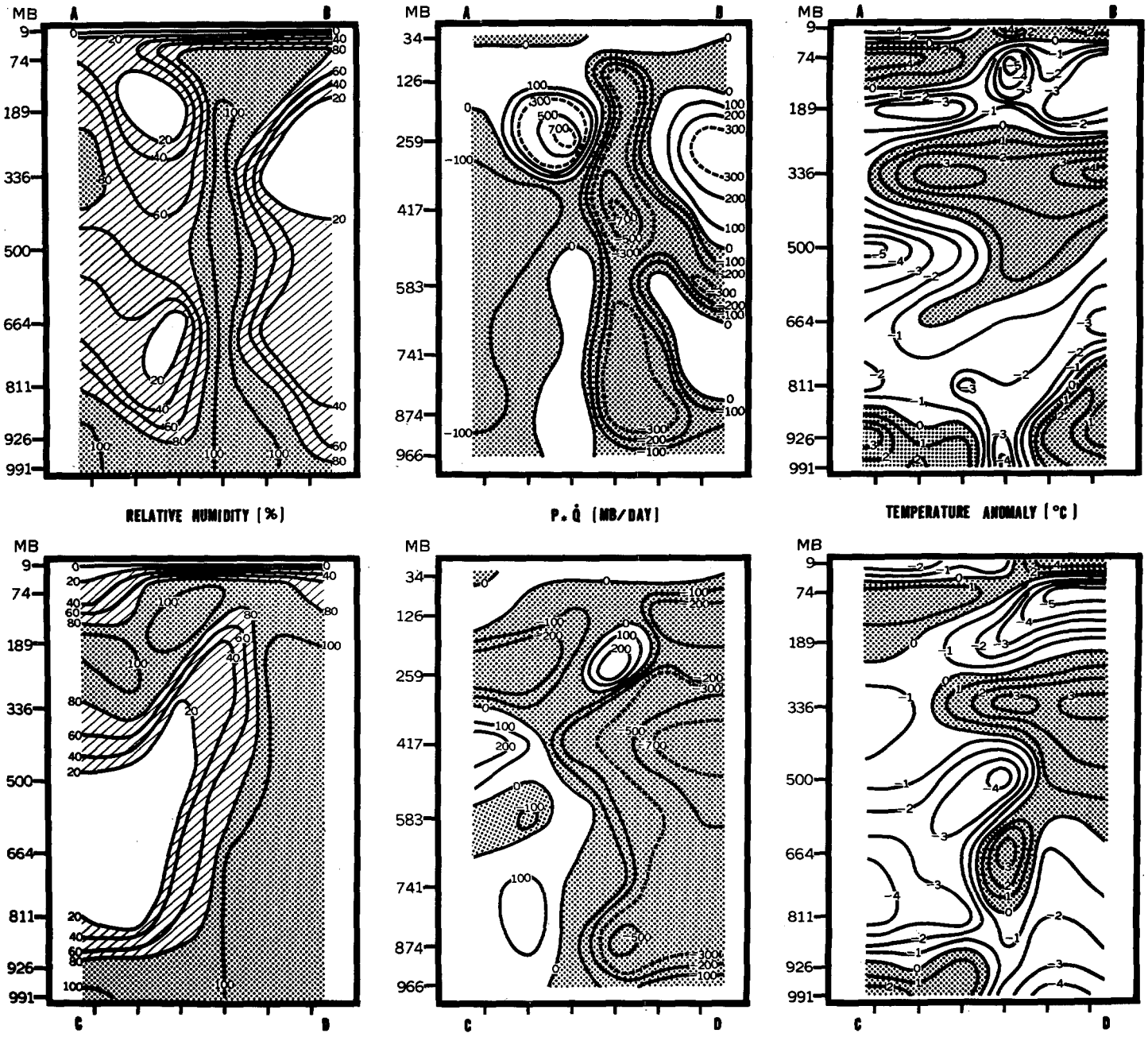

FIGURE 3.5.—Distributions of relative humidity, vertical P-velocity, and temperature anomaly on the cross section AB and CD (see 175th day map in fig. 3.2) are shown In the upper and lower part of the figure. The locations of grid points are indicated by pips at the bottom of each section.

potential energy in the Tropics of the moist model is significantly larger than the transfer between the eddy and zonal kinetic energies. This is not the case in the dry model atmosphere, as the upper half of figure 4.3 shows. These results are consistent with the latitudinal distributions of eddy kinetic energy mentioned above. It is noteworthy that the eddy kinetic energy in the tropical atmosphere of the moist model is at a maximum in the upper troposphere, as figure 9.2 of [6] shows.

Figure 4.3 shows that in the moist model atmosphere zonal kinetic energy is transferred into eddy kinetic energy. This result does not agree with observation (e.g., Oort [10]) except for the case of January 1963, which was pointed out by Wiin-Nielsen et al. [18]. According to our analysis of the moist model atmosphere, the intense direct cell in the Tropics involves an energy conversion from zonal available potential energy into zonal kinetic energy, thus maintaining the zonal kinetic energy against its transfer into eddy kinetic energy. In other words, the direct circulation is a very important factor in maintaining the subtropical jet stream in the moist model atmosphere. This apparently unrealistic result seems to be a direct consequence of the abnormal growth of the direct tropical cell which we discussed in Section 2. It is interesting,

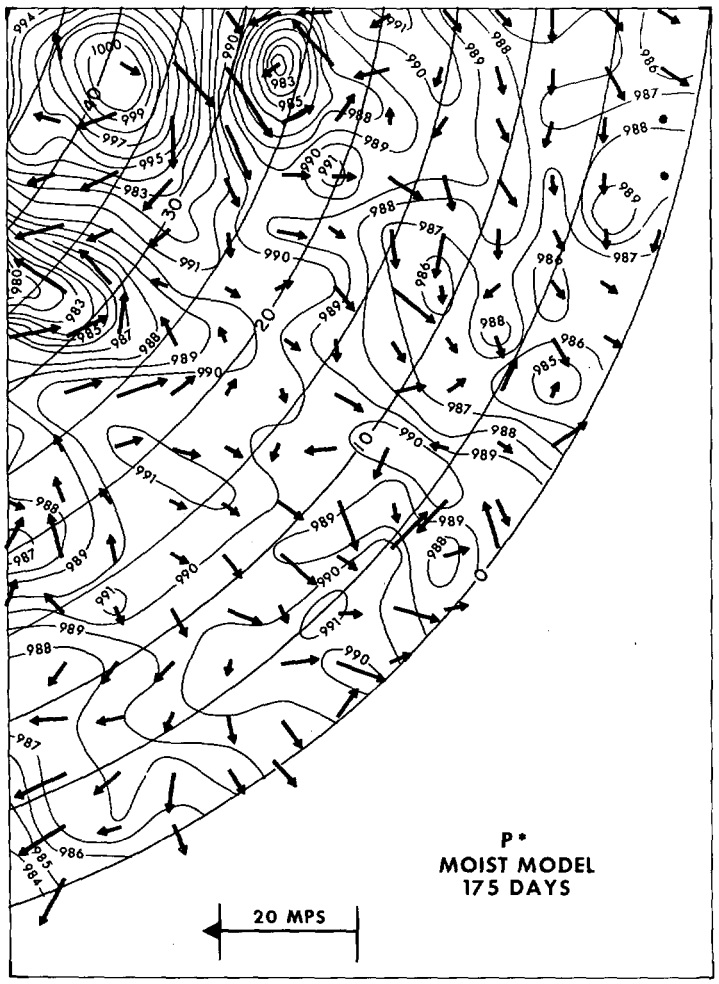

FIGURE 3.6.—Map of surface pressure and wind vector at level 9 ($P/P_*=0.991$) on 175th day of integration of moist model. Wind vectors have their tail at the grid point; the length of the vector (excluding arrowhead) is proportional to wind speed. Note that the mean sea level pressure of this model is systematically lower than that of the actual atmosphere.

however, that a recent study of Holopainen [2] suggests the importance of the direct cell in maintaining the subtropical jet stream during winter.

It then remains to determine how the eddy available potential energy is generated in the moist model Tropics. The latitude-height distributions of the generation of eddy available potential energy due to convection and condensation, that due to radiation, and that due to horizontal diffusion for both dry and moist models, are shown in figure 4.4. Also, the latitudinal distributions of the vertical integral of these generation terms are shown in figure 4.5. For comparison, the latitudinal distribution of the conversion of eddy available potential energy,

$$\frac{1}{g}\int_0^{P_*} \overline{\omega'\alpha'}^{\lambda}\, dP$$

that of the transfer from zonal to eddy available potential energy, $(A_Z \cdot A_E)$, are added to the same figure. As we explained on page 759 of [15], $(A_Z \cdot A_E)$ for each latitude can be expressed by the following formula:

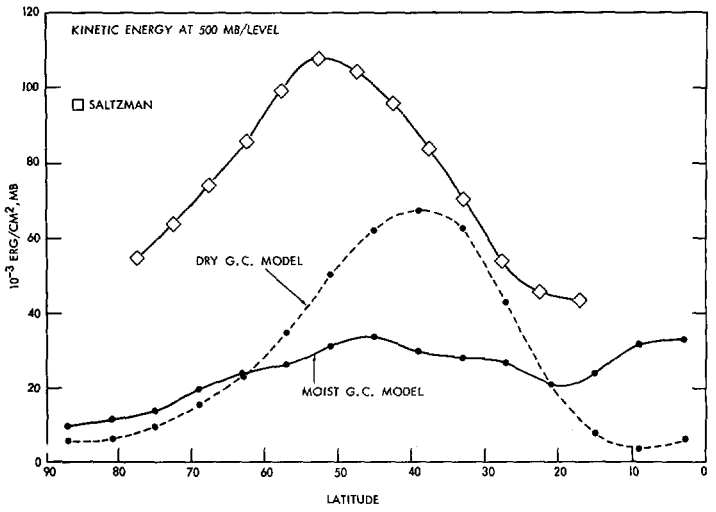

FIGURE 4.1.—The latitudinal distribution of eddy kinetic energy at the 5th model level of both the dry and moist general circulation models, and that at the 500-mb. level of the actual atmosphere obtained by Saltzman [14].

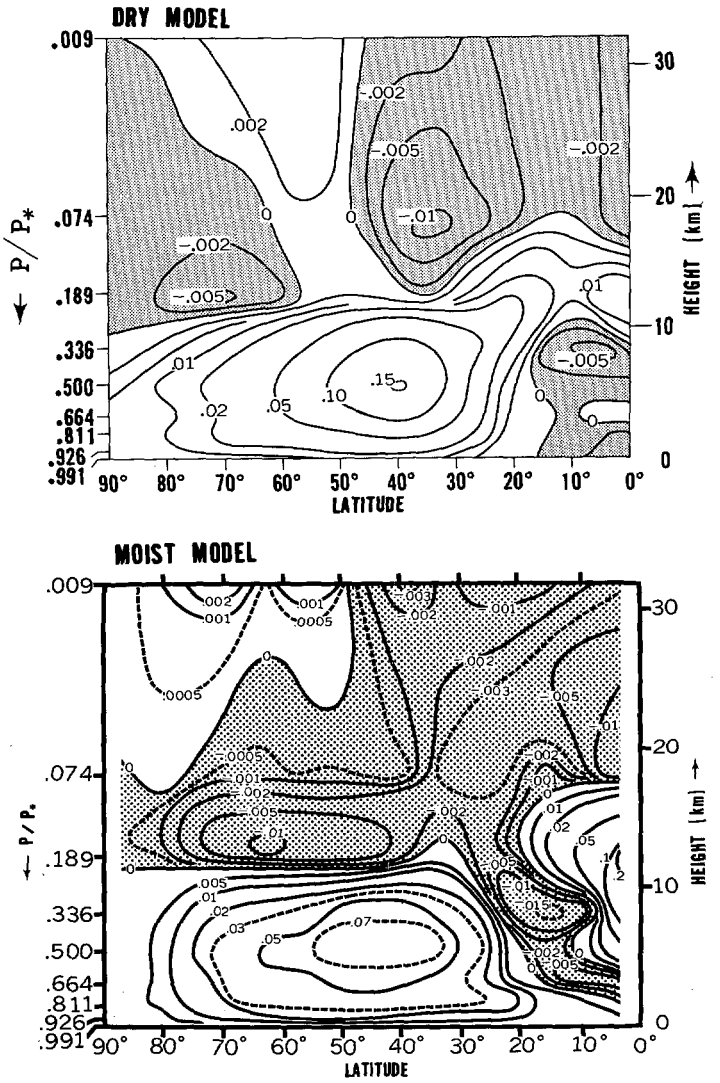

FIGURE 4.2.—Latitude-height distribution of the conversion of eddy available potential energy $-\overline{\omega'\alpha'}^{\lambda}$ for both dry and moist models (units: joule cm.$^{-2}$ mb.$^{-1}$ day^{-1}), averaged over 231st day to 300th day (dry model), 158th day to 177th day (moist model).

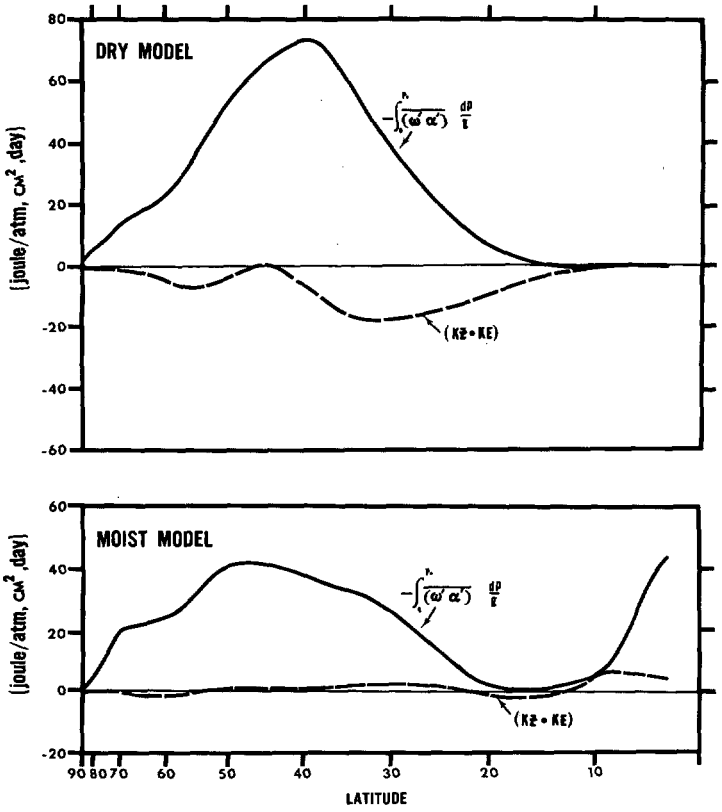

FIGURE 4.3.—Latitudinal distribution of the conversion of potential energy $\left(-\frac{1}{g}\int_0^{P*}\overline{\omega'\alpha'}^{\lambda}\alpha P\right)$ and the energy transfer from zonal to eddy kinetic energy for both dry and moist models, averaged over 264th day to 283d day (dry model), 158th day to 177th day (moist model).

$$(A_Z \cdot A_E) = -\frac{1}{g}\int_0^{P_*} \gamma \left[\overline{v'T'}^{\lambda}\frac{\partial(\overline{T}^{\lambda})''}{a\cdot\partial\theta} + \overline{\omega'T'}^{\lambda}\cdot\left(\frac{\partial(\overline{T}^{\lambda})''}{\partial P} + \kappa\frac{(\overline{T}^{\lambda})''}{P}\right)\right] dP \quad (4.2)$$

These figures show that in the moist model atmosphere, the generation of available potential energy which is due to condensation and convection predominates in the Tropics as well as in the middle latitudes. It compensates for the conversion into the eddy kinetic energy which we described in the previous paragraph. Further examination of figure 4.2 reveals that in the moist model atmosphere, the conversion of eddy available potential energy is at a maximum in the upper tropical troposphere. This is the location of the tropical cyclone warm cores resulting from convective adjustment, and is clearly seen in the upper-right-hand diagram of figure 4.4 as a maximum generation of eddy available potential energy due to convection and condensation. This tropical maximum is missing in the dry model because of the absence of warm-core structure.

Figure 4.6 shows the hemispheric energy budget of eddy available potential energy for both dry and moist model atmospheres. In the dry atmosphere, the prime source of eddy available potential energy is the transfer from zonal available potential energy, and convection contributes very little to the budget. In the moist model, condensation and convection generate as much eddy available potential energy as is transferred from zonal available potential energy.

The results of the analysis in this and the previous sections clearly demonstrate that *the conversion of eddy available potential energy generated by the heat of condensation is the major source of eddy kinetic energy in the Tropics of the moist model.*

5. SUMMARY AND CRITIQUE

The major features of interest in the model for the Tropics are as follows:

a. The lapse rate is super-moist-adiabatic in the lower troposphere and sub-moist-adiabatic above the 400-mb. level, in qualitative agreement with observation.
b. Because of the release of latent heat of condensation, the direct tropical meridional circulation cell is stronger than is the indirect cell in middle latitudes.
c. The cells of intense vertical motion develop in low latitudes and are responsible for the rainbelt in the model Tropics.
d. Synoptic-scale disturbances, such as convergence lines or weak cyclones, develop in the vicinity of the equator. They are usually accompanied by very intense upward motion.
e. The life cycle of many of the tropical disturbances is short, of the order of 1 to 3 days, and highly variable.
f. The kinetic energy of the synoptic-scale disturbances in the model Tropics is maintained against dissipation chiefly by the conversion from eddy available potential energy into eddy kinetic energy. The major source of eddy available potential energy in the model Tropics is its generation by the released heat of condensation.
g. In the model Tropics, humid towers of convective adjustment with moist adiabatic lapse rate occasionally reach as high as the level of the tropical tropopause. This occurs where intense upward motion predominates in the synoptic-scale disturbances. The heat of condensation in these humid towers compensates for the cooling by the meridional circulation and radiation in the upper tropical troposphere. It also creates the thermal structure of eddies favorable for the conversion of eddy potential energy, i.e., the warm core in the upper troposphere.
h. The relative humidity is at a maximum near the earth's surface and decreases with increasing altitude, reaching a tropospheric minimum at 400 mb., thereupon increasing again to a pronounced maximum just below the tropical tropopause.

Finally, it is necessary to add a critical remark. The characteristic scale of tropical disturbances is relatively small, and is barely resolvable by the grid size of 330 km. It is natural to wonder whether the characteristic scale

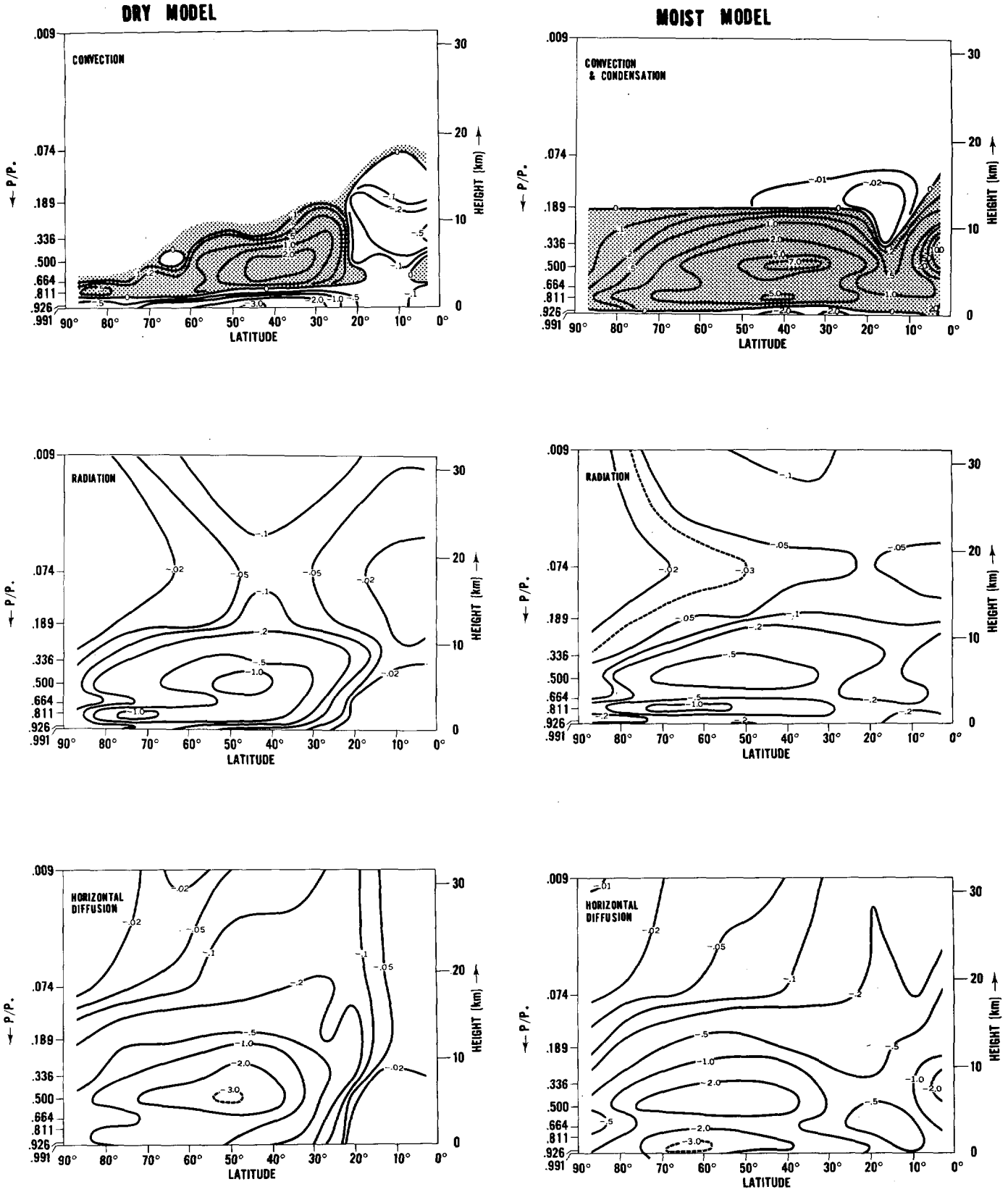

FIGURE 4.4.—Latitude-height distribution of the generation of eddy available potential energy due to various factors for both dry and moist model (units: 10^{-2} joule cm.$^{-2}$ mb.$^{-1}$ day^{-1}) averaged over 264th day to 283d day (dry model), 158th day to 177th day (moist model).

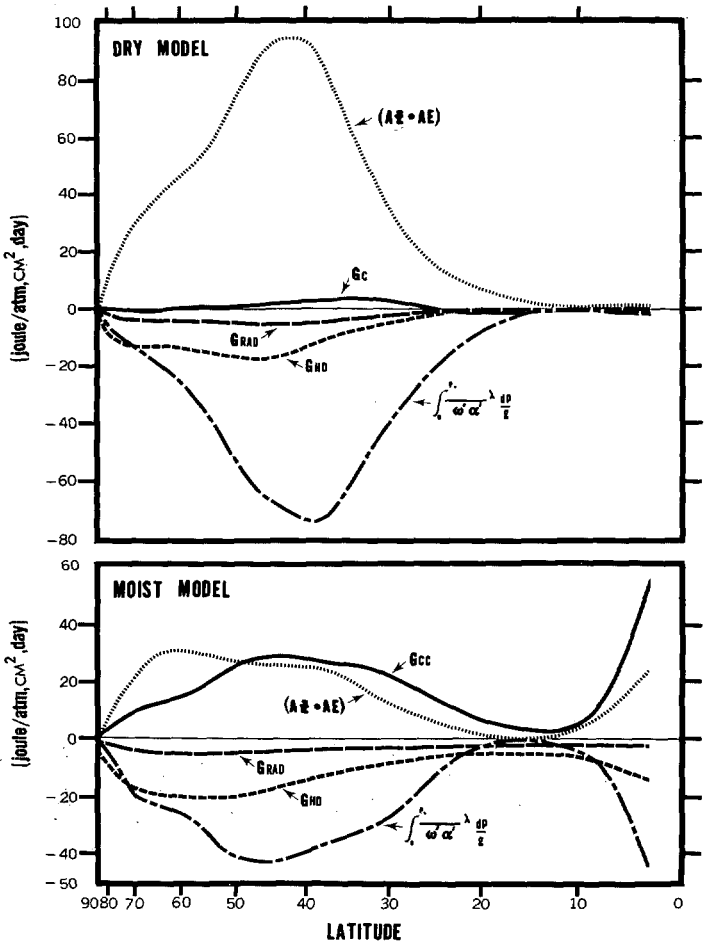

FIGURE 4.5.—Latitudinal distribution of the following factors: (1) vertical integral of the energy transfer from zonal to eddy available potential energy ($A_Z \cdot A_E$), (2) generation of eddy available potential energy due to convection (G_c; dry model only), (3) generation due to convection and condensation (G_{cc}; moist model only), (4) generation due to radiation (G_{RAD}), (5) generation due to horizontal diffusion (G_{HD}), and (6) conversion of eddy kinetic energy into eddy available potential energy. Averaged over 231st day to 300th day (dry model); 158th day to 177th day (moist model).

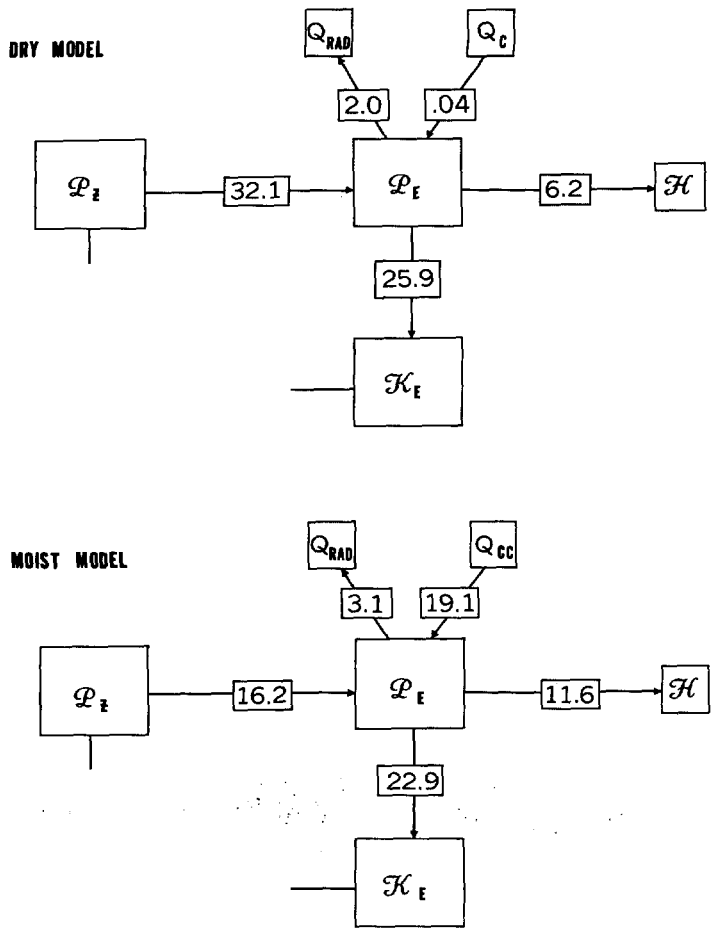

FIGURE 4.6.—Energy diagram showing the energy budget of eddy available potential energy. $\mathscr{P}_Z$ and $\mathscr{P}_E$ are zonal and eddy available potential energy respectively, $\mathscr{K}_E$ is eddy kinetic energy, Q^c or Q^{cc} denotes the change of available potential energy which is due to convection (dry model) or to condensation and convection (moist model); Q^R denotes that due to radiation. $\mathscr{H}$ denotes the change of available potential energy due to horizontal diffusion. The unit of energy transformation is 10^{-3} joule cm.$^{-2}$ mb.$^{-1}$ day^{-1}. Period of time mean: 264th day to 283d day (dry model); 158th day to 177th day (moist model).

is crucially controlled by the allowable resolution. However, preliminary analysis of a comparable high-resolution experiment (equatorial grid size 165 km.) indicates no significant change in the characteristic scale. Hence these results are not crucially resolution-determined. On the other hand, since they never attain great intensity, the possible passage to maturity may very well be resolution-controlled. This certainly is suggested by the observed relatively small size of the occasional low-latitude hurricane in contrast with the more prevalent tropical disturbance.

In the absence of an instability theory for these disturbances, we are deprived of the kinds of physical insights available for middle latitudes.

ACKNOWLEDGMENTS

We are grateful to Drs. Kikuro Miyakoda, Kirk Bryan, and Joanne M. Simpson for many useful suggestions and encouragement, to Mr. J. Leith Holloway, Jr., and Mrs. Catherine Hiland for completing the computer program, and to Mrs. Marylin Varnadore for her excellent technical assistance.

Appendix—List of Notations Used

T=Temperature
u=Zonal component of wind
v=Meridional component of wind

P=Pressure
P_*=Surface Pressure
$\omega=dP/dt$
g=Acceleration of gravity
θ=Latitude
a=Radius of the earth
$\kappa=\frac{R}{c_p}$
c_p=Specific heat under constant pressure.
R=Gas constant
$(K_z \cdot K_E)$=Vertical integral of the transfer from zonal to eddy kinetic energy as expressed by equation (4.1).
$(A_z \cdot A_E)$=Vertical integral of the transfer of zonal to eddy available potential energy as expressed by equation (4.2).

$$\gamma=-R\Big/\left(P\cdot\left(\frac{\partial\overline{T}^H}{\partial P}-\kappa\frac{\overline{T}^H}{P}\right)\right)$$

$\overline{\ }^{\lambda}$=Zonal mean
$\overline{\ }^{H}$=Hemispheric mean
$'$=Deviation from zonal mean
$''$=Deviation from hemispheric mean

Note: See the third term on the right hand side of equations (7.E.1) and (7.E.2) of reference [15] for the definition of zonal and eddy generation.

REFERENCES

1. M. I. Budyko, "Atlas Teplovogo Balansa Zemnogo Shara," *Mezhduvedomstvennyi Geofizicheskii Komitet pri Prizidium*, Akademiîa Nauk SSSR, Glavnaîa Geofizicheskaîa Observatoriîa imennii A. E. Voeĭkova, *Rezultaty*, 1964.
2. E. O. Holopainen, "On the Role of Mean Meridional Circulation in the Energy Balance of the Atmosphere," *Tellus*, vol. 17, No. 3, Aug. 1965, pp. 285–305.
3. F. Lipps, "Barotropic Stability Theory and Easterly Waves," 1966, (Unpublished manuscript).
4. J. London, "A Study of the Atmospheric Heat Balance," *Final Report* on Contract AF19(122)-165 (AFCRC-TR-57-287), Department of Meteorology and Oceanography, New York University, 1957, 99 pp.
5. J. S. Malkus, "Large-Scale Interactions" pp. 88–294 in *The Sea. Vol. I, Physical Oceanography*, M. N. Hill (ed.), Interscience Publishers, 1962.
6. S. Manabe, J. Smagorinsky, and R. F. Strickler, "Simulated Climatology of a General Circulation Model With a Hydrologic Cycle," *Monthly Weather Review*, vol. 93, No. 12, Dec. 1965, pp. 769–798.
7. H. J. Mastenbrook, "The Vertical Distribution of Water Vapor Over Kwajalein Atoll, Marshall Islands," *NRL Report 6367*, U.S. Naval Research Laboratory, Washington, D.C., Dec. 30, 1965.
8. Y. Mintz and J. Lang, "A Model of the Mean Meridional Circulation," *Final Report*, AF 19(122)-48, General Circulation Project, Paper No. VI, University of California at Los Angeles, 1955.
9. R. J. Murgatroyd, "Some Recent Measurements by Aircraft of Humidity up to 50,000 feet in the Tropics, and Their Relationship to Meridional Circulation," Proceedings of the Symposium on Atmospheric Ozone, Oxford, 20–25 July 1959, International Union of Geodesy and Geophysics, *Monograph* No. 3, Paris, 1960, 30 pp.
10. A. H. Oort, "On Estimates of the Atmospheric Energy Cycle," *Monthly Weather Review*, vol. 92, No. 11, Nov. 1964, pp. 483–493.
11. E. Palmén and L. A. Vuorela, "On the Mean Meridional Circulations in the Northern Hemisphere During the Winter Season," *Quarterly Journal of the Royal Meteorological Society*, vol. 89, No. 379, Jan. 1963, pp. 131–138.
12. H. Riehl, "Radiation Measurements Over the Caribbean During the Autumn of 1960," *Journal of Geophysical Research*, vol. 67, No. 10, Sept. 1962, pp. 3935–3942.
13. H. Riehl and J. S. Malkus, "On the Heat Balance in the Equatorial Trough Zone," *Geophysica*, vol. 6, No. 3/4, 1958, pp. 503–538.
14. B. Saltzman, "Spectral Statistics of the Wind at 500 mb.," *Journal of the Atmospheric Sciences*, vol. 19, No. 2, Mar. 1962, pp. 195–206.
15. J. Smagorinsky, S. Manabe, and J. L. Holloway, "Numerical Results From a Nine-Level General Circulation Model of the Atmosphere," *Monthly Weather Review*, vol. 93, No. 12, Dec. 1965, pp. 727–768.
16. E. Suomi and P. M. Kuhn, "An Economical Net Radiometer," *Tellus*, vol. 10, No. 1, Feb. 1958, pp. 160–163.
17. K. Telegadas and J. London, "A Physical Model of Northern Hemisphere Troposphere for Winter and Summer," *Scientific Report*, No. 1, Contract AF 19(122)-165, Research Division, College of Engineering, New York University, 55 pp.
18. A. Wiin-Nielsen, J. A. Brown, and M. Drake, "Further Studies of Energy Exchange Between the Zonal Flow and the Eddies," *Tellus*, vol. 16, No. 2, May 1964, pp. 168–180.
19. M. Yanai, "A Detailed Analysis of Typhoon Formation," *Journal of Meteorological Society of Japan*, Series II, vol. 39, No. 4, Aug. 1961, pp. 187–214.

[*Received November 3, 1966; revised January 24, 1967*]